S. Song

International Business Machine Corporation, Poughkeepsie, NY 12602

## M. M. Yovanovich

Microelectronics Heat Transfer Laboratory, Department of Mechanical Engineering.

#### F. O. Goodman

Department of Applied Mathematics and Department of Physics, University of Waterloo, Waterloo, Ontario, Canada

# Thermal Gap Conductance of Conforming Surfaces in Contact

Heat transfer through gas layers of contact interfaces formed by two microscopically rough surfaces is studied. Rarefied gas conduction between smooth parallel plates is examined with data obtained from the literature. Two important dimensionless parameters are introduced; one representing the ratio of the rarefied gas resistance to the continuum gas resistance, and the other representing gas rarefaction effects. Effects of gas rarefaction and surface roughness are studied in relation to the parallel plates case. It is proposed that the effective gap thickness at light loads may be estimate by a roughness parameter, the maximum peak height  $R_p$ . Experiments were performed to measure gap conductance for a number of Stainless Steel 304 pairs and Nickel 200 pairs over a range of roughnesses and gas pressures. Three different types of gases, helium, argon, and nitrogen, were employed as the interstitial gas. The comparison between the theory and the measured values of gap conductance shows excellent agreement.

#### 1 Introduction

Heat transfer through interfaces formed by the mechanical contact of two solids has many important applications, such as in heat exchangers, microelectronic-chip cooling, and nuclear fuel-temperature control. One of the fundamental (and perhaps most important) studies in contact heat transfer involves the contact of two surfaces that are flat but microscopically rough.

Typically heat transfer through contact interfaces is associated with the presence of interstitial gases/fluids. Under such conditions, the rate of heat transfer across the interfaces depends upon a number of parameters: thermal properties of solids and gases/fluids, surface roughness characteristics, applied mechanical load, microhardness characteristics of solids, etc. Because of the large number of parameters involved, numerous attempts by various researchers to model the thermal gap conductance have not been completely successful. While analytical models tend to neglect some of the important parameters, experimental correlations are valid only for limited ranges of these parameters (Shlykov, 1965; Veziroglu, 1967; Rapier et al., 1963). Often, the disagreement between the measured and predicted values of the conductance is found to be in the order of magnitude of the experimental values.

In the present paper various effects on the gap heat transfer are examined, using a rarefied gas kinetic theory and an accurate gap conductance model (Yovanovich et al., 1982). Also presented here are accurate gap conductance measurements obtained for interfaces formed by the contact of a bead-blasted surface and a smooth lapped surface. Helium, argon, and nitrogen were used as the interstitial gases with Stainless Steel 304 pairs and Nickel 200 pairs. Contact pressure was maintained at a very low level (0.4-0.6 MPa), so that the contribution of the contact conductance to the total (joint) conductance is small. Gas pressure was varied over 10 to 700 torr to study the effect of gas rarefaction on gap conductance. The model of Yovanovich et al. (1982) is verified using the experimental measurements. The comparison between the predicted and the measured conductance values shows excellent agreement.

# 2 Review of Contact Interface Heat Transfer

2.1 Conductance Definitions. Heat transfer through in-

Contributed by the Heat Transfer Division for publication in the JOURNAL OF HEAT FRANSFER. Manuscript received by the Heat Transfer Division April 1992; revision received February 1993. Keywords: Conduction, Electronic Equipment, Thermal Packaging, Associate Technical Editor: L. S. Fletcher.

terfaces formed by the contact of two nominally flat surfaces, when radiation effects are neglected, takes the following form:

$$Q_j = Q_c + Q_g \tag{1}$$

where  $Q_c$ ,  $Q_g$ ,  $Q_j$  are the rates of heat transfer through the solid contact spots, through the interstitial gas layer, and the total rate of heat transfer, respectively. The conductance is introduced in the same manner as the film coefficient in convective heat transfer:

$$h = \frac{Q/A_a}{\Delta T}$$

where h is the conductance,  $\Delta T$  is the effective temperature difference across the interface, and  $A_a$  is the apparent contact area

2.2 Gap Conductance. The earliest and simplest form of gap conductance models (Cetinkale and Fishenden, 1951; Fenech and Rohsenow, 1959; Laming, 1961; Shlykov and Ganin, 1964) assumes that the contact interface gap may be represented by two parallel plates separated by an effective gap thickness  $\delta$ . The gap conductance  $h_g$  is modeled as

$$h_g = \frac{k_g}{\delta} \tag{2}$$

where the effective gap thickness,  $\delta$ , depends upon the roughness characteristics of the two surfaces, the contact pressure and the microhardness. These models, however, ignore the effect of the contact pressure upon the gap thickness. The effective gap thickness  $\delta$  is estimated by correlating the gap conductance measurements in terms of the surface roughness, typically the sum of the centerline averages (CLA) of the two surfaces.

The magnitude of the effective gap thickness of contact interfaces is typically of the range  $0.1 < \delta < 100~\mu m$ . When the physical size of the gas layer, through which the gas conduction takes place, is comparable to the level of the gas molecular movement, the continuum assumption of the gas medium is no longer valid. This effect is commonly referred to as "rarefied gas" heat conduction.

This effect results in retardation of the heat transfer, and is often modeled in the form of a distance serially added to the physical heat flow path (Henry, 1964; Veziroglu, 1967; Yovanovich, 1982):

$$h_g = \frac{k_g}{\delta + M} \tag{3}$$

The gas parameter, M, depends upon the gas type, gas pressure and temperature, and the thermal accommodation coefficient (a measure of the energy exchange between the gas molecules and the solid surfaces). This parameter, which will be discussed in detail in Section 3, can vary in the order of the magnitude of the effective gap thickness,  $\delta$ .

The manner in which the gas rarefaction effect is modeled has not been agreed upon, as there appear to be a number of different approaches (Rapier et al., 1963: Lloyd et al., 1973; Garnier and Begej, 1979; Mentes et al., 1981; Loyalka, 1982). Furthermore, it is difficult to obtain an accurate estimate of the thermal accommodation coefficient (TAC), which is a parameter of critical importance in rarefield gas heat transfer. Most of the authors involved with contact interface gap heat transfer research have relied upon TAC measurements obtained in environments much different from the contact situations, and these estimates within themselves showed a great deal of uncertainties. There appears to be no previous serious effort taken to estimate TAC directly within the environment of the contact interface heat transfer.

Instead of making parallel-plate assumptions (Eqs. (2) and (3)), several authors (Shvets and Dyban, 1964; Shlykov, 1965; Popov and Krasnoborod'ko, 1975) took the approach of representing the geometry of the interface gap by correlating the surface height distributions obtained from several machined and ground surfaces. Dutkiewicz (1966) took a statistical approach by assuming that the roughness heights of the contact surfaces are distributed according to the Gaussian model, and presented tabulated results for the gap conductance predictions (with some restriction in the range of the surface height distributions).

Yovanovich et al. (1982), also assuming Gaussian distribution of the surface height, developed a gap conductance model in an integral form. In this model the effect on the deformation of the gap due to the contact pressure is taken into consideration. The development of the model is presented (briefly) here since this model is later modified and used extensively in the present work.

The integral model for the gap conductance, which is denoted in the present work as the YIGC (Yovanovich Integral Gap Conductance) model, takes into consideration the variation in the local gap thickness due to the surface roughness. The model assumes that the temperatures of the two surfaces in contact are uniform at  $T_1$  and  $T_2$ , and the entire interface gap consists of many elemental flux tubes of different thermal resistance. The resistances of these elemental flux tubes are

then connected in parallel to result in the overall gap conductance in an integral form:

$$h_g = \frac{k_g}{\sqrt{2\pi} \sigma} \int_0^\infty \frac{\exp[-(Y/\sigma - t/\sigma)^2/2]}{(t+M)/\sigma} d(t/\sigma)$$
 (4)

where t = length of the elemental flux tube or the local gap thickness;  $M = \text{gas parameter to be discussed in Section 3; } k_g$ = thermal conductivity of the gas; Y = mean plane separationdistance or effective gap thickness. The term t + M may be regarded as the effective heat flow distance of the local elemental flux tube.

# 3 Rarefied Gas Heat Transfer Between Parallel Plates

Gas conduction in the contact interface is a complex phenomenon mainly due to the statistical nature of the gap geometry. In addition, the uncertainty associated with the present understanding of rarefied gas heat transfer, which arises from the small size (comparable to the gas molecular movement level) of the gap thickness, makes it difficult to model the gap gas heat transfer accurately. Here, the case of the rarefied gas conduction between two smooth parallel plates is considered and the accuracy of a single parallel-plate, heat transfer model, which numerous researchers have incorporated into their contact interface gap conductance models, is verified with experimental data. The contact interface gas conductance may then be examined in relation with the parallel-plate case. During this analysis, a pair of important dimensionless parameters will be introduced.

3.1 Heat-Flow Regimes. Conduction heat transfer through a gas layer between two noncontacting parallel plates is commonly classified into four heat-flow regimes; continuum, temperature-jump, transition, and free-molecular (Springer, 1971). A convenient parameter that characterizes the regimes is the Knudsen number, defined as:

$$Kn = \frac{\Lambda}{d}$$
 (5)

where  $\Lambda$  is the molecular mean free path and d is the distance separating the two plates.

In the continuum regime (Kn << 1), the heat transfer between the plates takes place mainly through the collisions of the gas molecules. The rate of heat transfer in this regime is independent of the gas pressure, but varies with the gas temperature. Fourier's law of conduction can be used in this re-

#### Nomenclature -

 $A_a$  = apparent area of contact

CLA = centerline average surface

roughness

d = gap thickness

f = dimensionless term in Eq.(13)

G = dimensionless gap resistance

 $= \frac{k_g}{h_g d}$   $= \text{conductance} = \frac{Q/A_a}{\Delta T}$ 

 $Kn = Knudsen number = \Lambda/d$  $k_g$  = thermal conductivity of gas L = sample trace length

 $M = \text{gas parameter} = \frac{2 - \text{TAC}_1}{\text{TAC}_1} +$  $\frac{2-TAC_2}{TAC_2} \beta \Lambda$ 

= gas rarefaction parameter =

M/d

P = apparent contact pressure

 $P_g$  = gas pressure Pr = Prandtl number =  $c_p \mu/k$ 

Q = heat transfer rate

q = heat flux =  $Q/A_a$   $R_p$  = maximum peak height T = temperature

TAC = thermal accommodation coefficient

 $\Delta T$  = effective temperature differ-

ence across interface =  $T_1 - T_2$ 

t = local gap thickness

Y = mean plane separation, effective gap thickness

= ratio of specific heats =

 $\delta$  = effective gap thickness

 $\epsilon = \text{emissivity}$ 

 $\Lambda$  = molecular mean free path

 $\Lambda_0$  = at reference temperature and pressure

 $\sigma = \text{rms surface roughness}$ 

#### Subscripts

1, 2 = surfaces 1 and 2

c = contact

FM = free molecular

g = gas

j = joint

As the gas pressure is reduced, the intermolecular collisions become less frequent, and the exchange of energy between gas molecules and the plates starts to affect the heat transfer rate between the plates. Typically characterized by the Knudsen number range of  $0.01 < \mathrm{Kn} < 0.1$ , the heat flow under this conditions exhibits a "temperature-jump" behavior (Kennard, 1938). In this regime, the heat exchange of energy between the gas molecules and the plate wall is incomplete, and, as a result, a "discontinuity" of temperature develops at the wall-gas interface.

At the extreme end of very low gas pressure (or high gas temperature), intermolecular collisions are rare, and the essential mechanism of heat transfer in this regime is the exchange of energy between gas molecules and the plates. This heat-flow regime, typically with Kn > 10, is called the "free-molecular regime."

Between the temperature-jump and the free-molecular regimes is the "transition regime," in which intermolecular collisions and the energy exchange between the gas molecules and the plate walls are both important. The Knudsen number range for this regime is typically  $0.1 < {\rm Kn} < 10$ .

3.2 Simple Kinetic Theory Models. For the temperature-jump and the free molecular heat-flow regimes, there exist simple models for heat transfer through gases between two parallel isothermal plates. These models assume that the gas molecules are in thermal equilibrium and obey Maxwell's velocity distribution law. The heat transfer rate is modeled in terms of the gas molecular mean free path, and thus these models are sometimes referred to as "mean free path models."

When Maxwell's theory for temperature-jump distance is employed, the conduction between two parallel plates for the temperature-jump regime may be modeled as (Kennard, 1938):

$$q = \frac{k_g}{d+M} \left( T_1 - T_2 \right) \tag{6}$$

where  $T_1$  and  $T_2$  are the uniform temperatures of the two plates, and q is the heat flux. The gas parameter, M is defined as:

$$M = \left(\frac{2 - \text{TAC}_1}{\text{TAC}_1} + \frac{2 - \text{TAC}_2}{\text{TAC}_2}\right) \left(\frac{2\gamma}{\gamma + 1}\right) \left(\frac{1}{\text{Pr}}\right) \Lambda \tag{7}$$

where

 $TAC_1$ ,  $TAC_2$  = thermal accommodation coefficients corresponding to the gas-solid combination of plates 1 and 2, respectively;  $\gamma$  = ratio of specific heats; Pr = Prandtl number;  $\Lambda$  = molecular mean free path. The thermal accommodation coefficient (TAC) depends upon the type of gas-solid combination, and is, in general, very sensitive to the condition of the solid surface. It represents the degree to which the kinetic energy of a gas molecular is exchanged while in collision with the solid wall.

The gas parameter, M, which has the unit of length, represents in Eq. (6) the temperature-jump distances for the two plates. It is of the order of the gas mean free path, which in turn varies proportionally with the gas temperature and inversely with the gas pressure ( $\Lambda$  is inversely proportional to  $P_g$ ).

 $P_g$ ). The heat flux in the free-molecular regime was modeled by Knudsen (Kennard, 1938):

$$q_{FM} = \frac{k_g}{M} (T_1 - T_2) \tag{8}$$

It is observed from this model that the heat flow in the free-molecular regime is independent of the distance separating the two plates. Furthermore, the heat flux  $q_{FM}$  is inversely proportional to M and thus is directly proportional to the gas pressure.

The heat transfer mechanism of the transition regime is very complex, and there is no simple theory for this regime.

3.3 Interpolated Simple Kinetic Theory Model. Yovanovich (1982), in developing his approximate expression for  $h_g$  (Eq. (3)), assumed that Eq. (6) effectively represents the heat transfer for all four flow regimes. This assumption seems reasonable since for the continuum regime the gas parameter, M is negligibly small compared to d, and as the Knudsen number increases M begins to affect the term  $k_g/d + M$ . In the free-molecular regime, Eq. (6) effectively reduces to the free-molecular model, Eq. (8).

Various other researchers, in developing models for the gap conductance, have assumed this interpolated form for the rarefied-gas heat transfer. In the present work, Eq. (6) is referred to as the interpolated simple kinetic theory (ISKT) model. It will be seen in the following sections that this model provides an accurate representation of heat transfer for all conduction regimes of the parallel-plate configuration. Also, there exist some approximate solutions of the Boltzmann transport equation (Liu and Lees, 1961; Bassanini et al., 1967), and the ISKT model is in very good agreement with these solutions.

3.4 Comparison of ISKT Model With Experimental Data. The ISKT Model (Eq. (6)) may be written in terms of two dimensionless parameters as:

$$G = M^+ + 1 \tag{9}$$

where

$$G = \frac{k_g}{h_p d}$$

and

$$M^+ = \frac{M}{d}$$

The dimensionless gap resistance, G, may be interpreted as the ratio of the rarefied gas resistance to the continuum resistance. The dimensionless parameter,  $M^+$ , represents the degree of gas rarefaction, and accordingly it is here referred to as the rarefaction parameter. It is important to note that all experimental data discussed in this section essentially form one curve when normalized to these parameters.

Teagan and Springer (1968) made measurements of heat transfer between parallel plates using argon ( $0.06 \le \text{Kn} \le 5$ ) and nitrogen ( $0.03 \le \text{Kn} \le 0.5$ ). Two aluminum plates of 25.4 cm diameter were used with a gap distance of 0.13 cm separating them. Braun and Frohn (1976, 1977) used stainless steel plates of 27.5 cm diameter and 1 cm gap spacing to measure the heat transfer through helium and argon. The Knudsen number range covered for the helium measurements was  $10^{-4} \le \text{Kn} \le 2$  and for the argon,  $10^{-4} \text{Kn} \le 1$ .

Figure I shows the measured values of G in comparison with the predicted values of the ISKT model (Teagan and Springer reported their measurements in the form of  $Q/Q_{FM}$  against 1/Kn, and Braun and Frohn,  $Q/Q_{\text{continuum}}$  against 1/Kn). It is seen from the figure that, for the wide range (nearly five orders of magnitude) of  $M^+$  covered by these authors, the agreement between the predicted values of G and the measurements is excellent. It is important to observe that the ISKT model is also valid for the transition regime.

Two major conclusions concerning the rarefied-gas heat transfer between parallel plates may be drawn as a result of the preceding study:

- The ISKT model accurately predicts the heat flow rate for all conduction regimes.
- The heat flow rate, when normalized to G (dimensionless gap resistance), depends upon one parameter,  $M^+$  (rarefaction parameter).

#### 4 Contact Interface Gap Heat Transfer

4.1 Effect of Surface Roughness on Gap Conductance. Rarefied gas conduction between parallel plates may

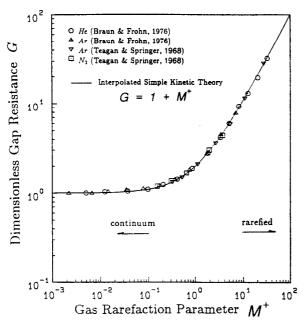


Fig. 1 Comparison of ISKT model with experimental data

be considered as the limiting case of the contact interface gas conduction as the surface roughness diminishes. The degree of the roughness effect upon the gap conductance has not been clearly understood. The integral gap conductance model (YIGC) provides an excellent description of the effect due to the surface roughness.

The YIGC model may be written for the dimensionless resistance, G, in terms of the gas rarefaction parameter,  $M^+$ , as:

$$G = \frac{k_g}{h_g Y} = \frac{\sqrt{2\pi}}{\int_0^\infty \frac{\exp\{-(Y/\sigma - t/\sigma)^2/2\}}{(t/\sigma)/(Y/\sigma) + M^+}} d(t/\sigma)$$
(10)

where G and  $M^+$  are defined in Eq. (9) with d replaced by the effective gap thickness Y.

The dimensionless resistance G, according to the YIGC model, depends on two parameters,  $M^+$  and  $Y/\sigma$ :

$$G = G(M^+, Y/\sigma) \tag{11}$$

As discussed in the previous section, the parameter  $M^+$  accounts for the gas rarefaction effect, and it is independent of surface roughness. According to the YIGC model, the surface roughness effect appears in the form of the ratio of the effective gap thickness to the rms roughness.

Figure 2 shows, in terms of the parameters G and  $M^+$ , the YIGC model (Eq. (10)) along with the ISKT model (Eq. (9)) of the parallel-plate gas conduction. The YIGC and ISKT models are essentially equivalent for the region of large  $M^+$  $(M^+ > 1)$ , and also for smooth surfaces (large  $Y/\sigma$ ). The parallel plates may be considered to be associated with negligible surface roughness, and thus the corresponding  $Y/\sigma$  value would be very large. Therefore, lower G values of YIGC model (compared to those of ISKT) may be interpreted to be due to the surface roughness effect. The surface roughness effect is significant only in the region of small  $M^+$  ( $M^+$ <1). Near the continuum regime (lower end of  $M^+$ ) the surface roughness effect, for the normal range of  $Y/\sigma$  (2.0 \le Y/\sigma \le 4.0) is seen to produce about 40 percent enhancement in the gap conductance (compared to the perfectly smooth surface with the same effective gap thickness Y).

The gas rarefaction effect, which depends upon the rarefaction parameter  $M^+$  is shown as an increase in the dimensionless resistance G. For the range  $M^+ > 1$ , the gap heat

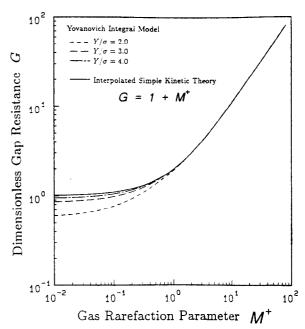


Fig. 2 YIGC model in terms of G and M<sup>+</sup>

transfer does not appear to depend upon the surface roughness, and thus the gap conductance in this regime (and only in this regime) may be effectively estimated as:

$$h_g = \frac{k_g}{M + Y} \tag{12}$$

The analysis presented in this section based on the YIGC model reveals several important aspects of the gap conductance:

- The dimensionless gap resistance G represents the relative magnitude of the gap resistance in reference to the resistance associated with the gas layer (in the continuum conduction regime) between the parallel plates.
- The gap conductance, when normalized to G, is influenced by two effects: the gas rarefaction and the surface roughness. These effects are characterized by the dimensionless parameters M<sup>+</sup> for the gas rarefaction and Y/σ for the surface roughness.
- In the region  $M^+ > 1$ , the influence on the gap conductance of the surface roughness effect is negligible.

4.2 Simplified Expression for YIGC Model. Equation (10) is in an integral form, and its evaluation requires numerical integration. The integral was correlated by the first author to yield the following simple expression:

$$G(M^+, Y/\sigma) = f + M^+ \tag{13}$$

where

$$f = 1 + \frac{0.304}{(Y/\sigma)(1+M^+)} - \frac{2.29}{\{(Y/\sigma)(1+M^+)\}^2}$$

For the range  $2.5 \le Y/\sigma$  and  $0.01 \le M^+$ , the maximum difference in G values computed by the simple expression and the integral model (Eq. (10)) is about 2 percent. When  $M^+$  is very small (continuum regime), Eq. (13) becomes independent of  $M^+$  and reduces to:

$$G \simeq f_{\text{continuum}}$$
 (14)

where

$$f_{\text{continuum}} = 1 + \frac{0.304}{Y/\sigma} - \frac{2.29}{(Y/\sigma)^2}$$

This expression should be useful for applications where the interstitial fluid is liquid or grease.

#### 5 Effective Gap Thickness

A critical part of the gap conductance model is to predict the effective gap thickness of the gas/fluid layer in the contact interface accurately. This is a difficult task mainly because there are many parameters that influence the gap thickness, e.g., surface roughness characteristics, mechanical load, and microhardness characteristics. Here the effective gap thickness is defined as the separation distance of the mean planes between two surfaces, and is given the symbol Y. The effective gap thickness Y increase with the surface roughness, and it decreases with increase in the mechanical load.

Yovanovich et al. (1982) developed an effective gap thickness model, which takes into consideration the effects of surface roughness and the mechanical load. The model assumes that the distribution of the surface roughness height is Gaussian, and inherent in this assumption is that the range of the surface height is unbounded. This implies that, hypothetically, under an extremely light load condition the effective gap thickness Y would take on a very large value. In reality this is not valid, especially for the contact of a rough and a smooth surface, because under the zero-load (or near the zero-load) condition the effective gap thickness for the contact of the real surface would correspond to the largest value of the surface height (from the mean plane of the rough surface), which would be the height of the highest peak. The increase of mechanical load from the zero-load condition results in the reduction of the effective gap thickness, and thus the increase in the gap conductance (Song et al., 1989).

In the present work, the contact of a rough and a smooth surface under very light mechanical load is considered, and the effective gap thickness is estimated as the maximum peak height of the rougher surface. The maximum peak height,  $R_p$ , is defined (Dagnall, 1980) as the height of the highest point of the profile above the mean line within the trace length L. The maximum peak height is an extreme value characteristic of the surface roughness, and thus, unlike other roughness parameters, such as the rms height  $(\sigma)$  or the centerline average height (CLA), it depends upon the trace length  $(R_p)$  increases with L). Therefore for an estimate of the effective gap thickness at light loads,  $R_p$  should be measured based on sufficiently long trace lengths.

The normalized value of the maximum peak height,  $R_p/\sigma$ , is of great interest in the present work, since it provides an estimate for the relative effective gap thickness  $(Y/\sigma)$  at light mechanical pressure. There appears to be a trend that  $R_p/\sigma$  of real surfaces in general decreases with increase in surface roughness (Rupert, 1959; Tsukada and Anno, 1975).

## 6 Experimental Program

6.1 Test Apparatus. A pyrex bell jar and a base plate enclose the test column (Fig. 3) consisting of the heater block, the heat meter, the upper and lower test specimens, the heat sink, and the load cell. The gas pressure inside the chamber was controlled by the vacuum system, which consisted of a mechanical pump connected in series with an oil diffusion pump. This system provided a vacuum level lower than 10<sup>-3</sup> torr. The brass heater block with two pencil-type heaters provided the maximum combined power of 200 W. Cooling was accomplished with an aluminum cold plate, which, in turn, was chilled by a closed-loop thermobath. Axial load was applied to the test column via a level system, which was activated by a diaphragm-type air cylinder. The mechanical load was measured by a calibrated load cell. A metal diaphragm type of gage was used to measure gas pressure inside the test chamber. The uncertainty associated with the gas pressure measurement was within 0.5 torr. Temperature measurements were made with 30 gage type "T" copper-constantan thermocouples. Data acquisition and reduction were performed under

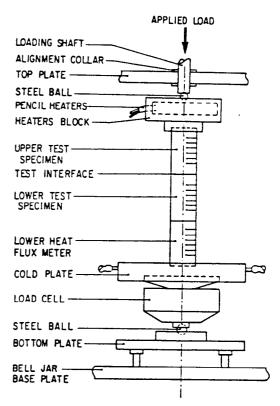


Fig. 3 Experimental setup

the control of a PC. The mechanical loads and the heater levels were adjusted through the computer.

6.2 Test Specimens and Gases. Test specimens of Stainless Steel 304 and Nickel 200 (Table 1) were prepared from commercial bars. The specimens were machined to cylindrical shape of 25 mm diameter and 45 mm long. For each specimen, six holes of 0.64 mm diameter and 2.5 mm deep were drilled for the thermocouples. These holes were located 5 mm apart with the first one 10 mm from the contact surface.

The contact surfaces were prepared by bead-blasting. A Talysurf profilometer was used to measure various surface roughness parameters. The roughness parameters estimated from the profilometer were as follows:  $\sigma = \text{rms}$  surface roughness; CLA = centerline average surface roughness;  $R_p = \text{maximum}$  peak height roughness. Typically, three to six traces were randomly selected, and the roughness parameters were measured over 1 cm trace lengths.

Three different types of gas, helium, argon, and nitrogen, were used in the experiments. Thermal conductivity correlations used for the gases were as follows:

Helium
$$k_g \text{ (W/m·K)} = 0.145 + 3.24 \times 10^{-4} \text{T for } 27 \le T \le 400^{\circ} \text{C}$$

$$Argon$$

$$k_g \text{ (W/m·K)} = 0.0171 + 4.05 \times 10^{-5} \text{T for } 20 \le T \le 400^{\circ} \text{C}$$

$$Nitrogen$$

$$k_g \text{ (W/m·K)} = 0.0250 + 5.84 \times 10^{-5} \text{T for } 27 \le T \le 400^{\circ} \text{C}$$
(17)

The thermal conductivity expressions for helium and nitrogen are the correlations of Hegazy (1985) and for argon the tabulated values of Gandhi and Saxena (1968) were correlated by the first author. The values of TAC for He, Ar, and  $N_2$  were

Table 1 Ranges of parameters for experiments

Table 1 Ranges of parameters for experiments					
Parameters	Exp. No. 1	Exp. No. 2	Exp. No. 3	Exp. No. 4	
Specimens $\sigma$ ( $\mu$ m) $R_p/\sigma$ $h_c$ ( $W/m^2 \cdot ^\circ$ C) $h_g/h_c$ ( $W/m^2 \cdot ^\circ$ C) $h_g/h_c$ ( $H_g/h_c$	SS 304 1.53 5.55 3.63 452 $\pm$ 25 711–9660 1.57–21.4 9.4–710.9 0.019–4.2 0.60 $\pm$ 0.02 172 $\pm$ 4 5.8–85.5 27.7–58.7	SS 304 4.83 14.7 3.04 241±3 460-5150 1.91-21.4 9.5-665.0 0.0078-1.6 0.47±0.02 168±4 6.7-105.9 34.4-55.5	Ni 200 2.32 8.61 3.71 1130 ± 30 625-17900 0.553-15.8 9.6-697.7 0.013-2.6 0.52 ± 0.02 170 ± 3 5.5-39.9 52.7-104.9	Ni 200 11.8 30.6 2.59 725±30 417-7830 0.575-10.8 9.4-699.7 0.0034-0.76 0.38±0.01 172±4 12.2-63.8 55.9-104.1	

 $\sigma = \sqrt{\sigma_1^2 + \sigma_2^2}$ 

Table 2 Properties of gases

14	DIC 2 1.0P		
Gas	γ	Pr	$\Lambda_0 (\mu m)$
Helium Argon Nitrogen	1.67 1.67 1.41	0.67 0.67 0.69	0.186 0.0666 0.0628

Note:  $\Lambda_0$  values (Kennard, 1938) are at 288 K and 760 torr.

estimated according to a method proposed by Song and Yovanovich (1989).

The estimated values of TAC are 0.55, 0.90, and 0.78 for He, Ar, and  $N_2$ , respectively. The values of other relevant properties of the gases (ratio of specific heats, Prandtl number, and molecular mean free path) are shown in Table 2.

## 6.3 Experimental Procedures

Specimen Placement. For the stainless steel tests, two specimens, one with smooth and the other with bead-blasted surfaces, were employed for each test. The specimen with the bead-blasted surface was always placed on top of the smooth-surface specimen.

For the nickel tests, an Armco iron heat meter was placed underneath the smooth-surfaced specimen in order to raise the mean interface contact temperature to the level compatible to that of the stainless steel tests. The placement of the Armco iron also provided a means to confirm correct measurement of heat flow rates through the upper and lower specimens. The test column was shielded with aluminum foil, and insulated with about a 2-cm-thick layer of quartz wool, which was then covered again with aluminum foil.

Test Order. All tests under a gas environment (helium, argon, and nitrogen) were preceded by at least one measurement under vacuum.

In general, the tests were performed in the following order:

- (a) at least one vaccum test
- (b) series of helium tests at various gas pressure
- (c) vacuum test
- (d) series of nitrogen tests
- (e) vacuum test
- (f) series of argon tests

Occasionally, different permutations of the above test orders were tried, so that any possible effect on gap conductance of the test order for the different gases may be observed.

Joint Conductance Measurements. The joint conductance  $h_j$  was obtained from the temperature measurements of the specimens according to its usual definition:

$$h_j = \frac{Q/A_a}{\Delta T} \tag{18}$$

The heat transfer rate Q was taken as the average value of the heat flow rates of the upper and lower specimens. The interface temperature difference  $\Delta T$  was obtained from the difference in the extrapolated values of the temperature of the interface from least-square fitted temperature distributions within the two specimens.

The time duration between the establishment of the control parameters (gas pressure, load level, and heater level) and the measurement was typically 30-120 minutes. In the case of "cold" starts, at least three hours of elapse time were allowed before the first measurement.

Before each measurement was made, the change with time of joint conductance and the temperature readings from the thermocouples were closely monitored.

Gap Conductance Measurements. Gap conductance measurements reported in the present work are based on the difference of the values of joint conductances obtained for the gas-environment and vacuum tests. In terms of the conductance coefficients, measured values of  $h_g$  correspond to the following:

$$(h_g)_{\text{measured}} = (h_j)_{\text{gas}} - (h_j)_{\text{vacuum}}$$
 (19)

where

$$(h_j)_{gas} = h_j$$
 measured in a gas environment  
 $(h_j)_{vacuum} = h_j$  measured in a vacuum

This is the most common means by which experimental values of  $h_g$  are estimated. The values of  $h_g$  obtained according to Eq. (19) most accurately reflect the actual values of  $h_g$  when the contribution of the heat transfer through the contacting solid spots is small compared to that through the gas layer. Throughout this work, measured values of  $h_g$  will refer to the values obtained according to Eq. (19). The effective gap thickness Y was estimated by the maximum peak height  $R_p$  of the rougher surface of each specimen pair, as discussed in Section

6.4 Experimental Uncertainty. The error associated with the joint conductance measurement (Eq. (18)) is attributed mainly to the uncertainty in the estimate of the heat transfer rate Q across the contact interface. The heat loss, as estimated by the difference between the heat transfer rates through the upper and lower specimens, was as great as 21 percent of the mean value for the tests with helium as the interstitial gas. The heat loss for the tests with nitrogen was much less (maximum 11 percent), and was the least with argon (maximum 8 percent). The mean value of the heat transfer rates between the upper and the lower specimen was used as the estimate for Q in the present work, and this implies that the maximum uncertainty associated with the  $h_j$  measurement is estimated to be less than 10 percent for the tests with helium, 6 percent with nitrogen, and 4 percent with argon. For vacuum tests  $(h_j)_{\text{vacuum}}$  is estimated to be less than about 3 percent.

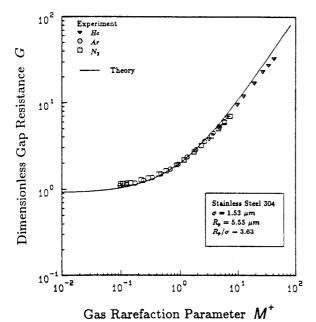


Fig. 4 Dimensionless gap resistance results of Exp. No. 1

The radiation heat exchange across the contact interface is estimated to be less than 1 percent of the total heat transfer rate. The radiative component of the joint conductance, estimated by assuming two isothermal parallel plates  $(T_1)$  and  $(T_2)$ , diffusive grey surfaces with emissivities  $\epsilon_1 = \epsilon_2 = 0.2$ , is about 0.9 percent for the case of the lowest  $h_j$  measurement under a vacuum.

#### 7 Experimental Results

Stainless Steel 304 Pair Experiments. The roughness of the bead-blasted surface for Exp. No.  $1(\sigma = 1.53 \mu m)$  is the lowest of all bead-blasted surfaces. Due to the low combined roughness of the surface pair, an effective gap thickness Y as low as 5.6 µm was obtained. Thus, it was possible to achieve a high degree of gas rarefaction (Knudsen number as high as 4.2 for the helium test at  $P_g = 9.4$  torr). When the results of all helium, argon, and nitrogen tests are combined, the gap conductance tests for this sample pair span a wide Knudsen number range, 0.019 < Kn < 4.2, which nearly covers the continuum, temperature-jump, and transition heat conduction regimes. Figure 4 shows the comparison between the measured and the predicted values of the gap conductances in the form of the dimensionless resistance G over a range of the rarefaction parameter  $M^+$ . It is observed from the figures that in terms of the two dimensionless parameters  $M^+$  and G, the test results for the three gases essentially form a single curve and there is no longer the need to distinguish between different gases. The test results of this specimen pair combined with the three different gases cover three orders of magnitude range of the rarefaction parameter  $M^+$ , and for this range, the measured values of the gap conductances (or G) agree well with the predicted values (Eq. (13)).

The Knudsen number range covered by Exp. No. 2 ( $\sigma = 4.83 \ \mu m$ ) is 0.0078 < Kn < 1.6, whose lower end would be considered to be well within the continuum regime. The dimensionless gap resistance results are shown in Fig. 5.

Nickel 200 Pair Experiments. The thermal conductivity of nickel is about 3.5 (at 170°C) times that of stainless steel. Thus the contribution to the joint conductance of the contact conductance is significantly greater than that of the stainless steel contact of similar conditions. The ratio of measured values of the joint and contact conductances varies from 0.65 for argon at 11 torr to 16.2 for helium at 640 torr. For both argon and

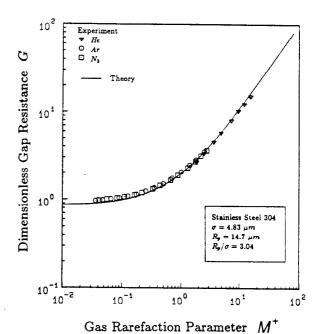


Fig. 5 Dimensionless gap resistance results for Exp. No. 2

ee

ce

<u>1e</u>

ol

1e

of ed

1e

S-

f-

эe

en

ıg

r.

ne

ае

n

th

₽₫

er

эd

ne

he

he

m

t).

er

he

<u>ty</u>

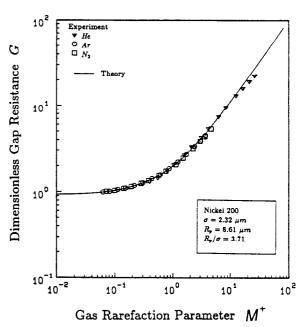


Fig. 6 Dimensionless gap resistance results for Exp. No. 3

nitrogen measurements, the contact conductance contributed at least 30 percent of the joint conductance. The gap conductance results are in excellent agreement, as shown in Fig. 6. Even for the argon measurements at  $P_g = 11$  torr ( $M^+ = 4.0$ ), where the gap conductance is approximately half of the contact conductance, the agreement is very good.

The surface roughness for Exp. No. 4 ( $\sigma=11.8~\mu m$ ) is the highest of all bead-blasted surfaces. Because of the high value of  $\sigma$  (thus large Y), the lower end of the Knudsen number range of the test is situated well within the continuum regime. The value of  $R_p/\sigma$  (and thus  $Y/\sigma$  estimate) for the sample pair is 2.59 (compared to 3.63, 3.04, and 3.71 for the samples in Exp. Nos. 1-3, respectively). At this low level of  $Y/\sigma$  the effect on the gap conductance due to the nonuniformity of the local heat flow length becomes significant, and this experiment provides a test to verify the modeling of the surface roughness effect. The gap conductance results (Fig. 7) are in excellent agreement with the theory. The Knudsen number of the argon

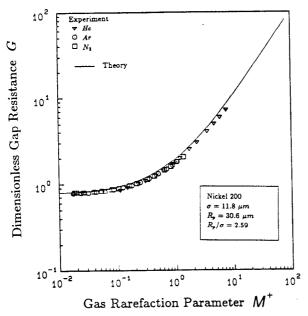


Fig. 7 Dimensionless gap resistance results for Exp. No. 4

test at  $P_g = 670 \text{ torr } (M^- = 0.018 \text{ in the figure}) \text{ is } 0.0034 \text{ and}$ the corresponding heat-flow regime may be considered continuum. At this point the predicted and the measured values of G are in excellent agreement at 0.80. This seems to suggest that the enhancement in the gap conductance due to the nonuniformity of the local heat flow length (arising from the surface roughness) for the particular test surface pair is about 20 percent. Thus the surface roughness effect, as modeled by the present gap conductance theory, may be significant and should not be ignored.

#### Summary

The accuracy of the simple model (ISKT) for predicting the rarefied gas heat transfer between two smooth parallel plates was verified through available experimental data. Two important dimensionless parameters, G and  $M^+$ , were introduced. Using the existing gap conductance model (YIGC), two predominant effects on gap conductance, gas rarefaction and surface roughness, were discussed. For light-load conditions it was proposed that the maximum peak height  $R_p$  may be used to estimate gap thickness.

Gap conductance measurements for light contacts of Stainless Steel 304 pairs and Nickel 200 pairs with helium, argon, and nitrogen as interstitial gases are presented. The measurements were obtained over wide ranges of surface roughness and gas pressure. The measured values of gap conductance are in excellent agreement with the predictions that use the roughness parameter  $R_p$  as the estimate for the light-load effective gap thickness. It was also demonstrated that for a given contact interface geometry (i.e., specified roughness and mechanical load) the gap conductance measurements of various gases, when normalized to G, depend upon only one parameter  $M^+$ .

### Acknowledgments

The authors gratefully acknowledge the assistance of Ms. B. G. Herles for preparation of the manuscript.

#### References

Bassanini, P., Cercignani, C., and Pagani, C. D., 1967, "Comparison of

Kinetic Theory Analysis of Linearized Heat Transfer Between Parallel Plates," Int. J. Heat Mass Transfer, Vol. 10, pp. 447-460.

Braun, D., and Frohn, A, 1976, "Heat Transfer in Simple Monatomic Gases and in Binary Mixtures of Monatomic Gases," Int. J. Heat Mass Transfer, Vol. 19, pp. 1329-1335.

Braun, D., and Frohn, A., 1977, "Heat Transfer in Binary Mixtures of Monatomic Gases for High-Temperature Differences and for a Large Knudsen Number Range," Rarefied Gas Dynamics, J. L. Potter, ed., pp. 149-159.

Cetinkale, T. N., and Fishenden, M., 1951, "Thermal Conductance of Metal Surface in Contact," Proc. of General Discussion on Heat Transfer, IMechE, London, pp. 271-275.

Dagnall, H., 1980, Exploring Surface Texture, Rank Taylor Hobson, United

Dutkiewicz, R. K., 1966, "Interfacial Gas Gap for Heat Transfer Between Two Randomly Rough Surfaces," Proc. of the 3rd Int. Heat Transfer Conf., Vol. 4, pp. 118-126.

Fenech, H., and Rohsenow, W. M., 1959, "Thermal Conductance of Metallic Surfaces in Contact," Report, Heat Transfer Lab., M.I.T., Cambridge, MA. Gandhi, J. M., and Saxena, S. C., 1968, "Correlated Thermal Conductivity Data of Rare Gases and Their Binary Mixtures at Ordinary Pressures," J. of

Chemical and Engineering Data, Vol. 13, No. 3, pp. 357-367. Garnier, J. E., and Begej, S., 1979, "Ex-reactor Determination of Thermal Gap and Contact Conductance Between Uranium Dioxide: Zircaloy-4 Inter-

faces," U.S. Nuclear Regulartory Commission Report. Hegazy, A. A., 1985, "Thermal Contact Conductance of Rough Surfaces: Effect of Surface Micro-hardness Variation," Ph.D. Thesis, Department of

Mechanical Engineering, University of Waterloo, Ontario, Canada. Henry, J. J., 1964, "Thermal Contact Resistance," Ph.D. Thesis, M.I.T., Cambridge, MA

Kennard, E. H., 1938, Kinetic Theory of Gases, McGraw-Hill, New York-

Laming, L. C., 1961, "Thermal Conductance of Mechanical Contacts," ASME

Int. Heat Transfer Conf., Part 1, No. 8, pp. 65-76.

Liu, C. Y., and Lees, L., 1961, "Kinetic Theory Description of Plane Compressible Couette Flow," Rarefied Gas Dynamics, L. Talbot, ed., Academic

Press, New York, pp. 391-428. Lloyd, W. R., Wilkins, D. R., and Hill, P. R., 1973, "Heat Transfer in

Multicomponent Monatomic Gases in the Low, Intermediate and High Pressure Regime," presented at the Nuclear Thermonics Conference.

Loyalka, S. K., 1982, "A Model for Gap Conductance in Nuclear Fuel Rods," Nuclear Technology, Vol. 57, pp. 220-227

Mentes, A., Veziroglu, T. N., Samudrala, R., Sheffield, J. W., and Williams, A., 1981, "Effects of Interface Gases on Contact Conductance," presented at the AIAA 19th Aerospace Sciences Meeting, St. Louis, MO, Jan. 12-15.

Popov, V. M., and Krasnoborod'ko, A. I., 1975, "Thermal Contact Resistance in a Gaseous Medium," Inzhenero-Fizicheskii Zhurnal, Vol. 28, No. 5, pp. 875-883.

Rapier, A. C., Jones, T. M., and McIntosh, J. E., 1963, "The Thermal Conductance of Uranium Dioxide/Stainless Steel Interfaces," Int. J. Heat Mass Transfer, Vol. 6, pp. 397-416.

Rupert, M. P., 1959, "Confusion in Measuring Surface Roughness," Engineering, Oct., pp. 393-395.

Shlykov, Yu. P., and Ganin, Ye. A., 1964, "Thermal Resistance of Metallic

Contacts," Int. J. Heat Mass Transfer, Vol. 7, p. 921-929. Shlykov, Yu. P., 1965, "Calculating Thermal Contact Resistance of Machined Metal Surfaces," Teploenergetika, Vol. 12, No. 10, pp. 79-83.

Shvets, I. T., and Dyban, E. P., 1964, "Contact Heat Transfer Between Plane

Metal Surfaces," Int. Chemical Engineering, Vol. 4, No. 4, pp. 621-624. Song, S., and Yovanovich, M. M., 1989, "Contact Interface Gas Heat Transfer: A Method of Measuring Thermal Accommodation Coefficient," Proceedings of 9th Annual International Electronics Packaging Conference, San Diego, Ca., Sept. 10-14.

Song, Y., Yovanovich, M. M., and Nho, K., 1989, "Thermal Gap Conductance: Effect of Gas Pressure and Mechanical Load," AIAA Paper No. 89-0429

Springer, G. S., 1971, "Heat Transfer in Rarefied Gases," Advances in Heat Transfer, T. F. Irvine and J. P. Hartnett, eds., Academic Press, Vol. 7, pp. 163-218.

Teagan, W. P., and Springer, G. S., 1968, "Heat-Transfer and Density-Distribution Measurements Between Parallel Plates in the Transition Regime,' Physics of Fluids, Vol. 11, No. 3, pp. 497-506.

Tsukada, T., and Anno, Y., 1975, "An Evaluation of Machined Surface Topography (2nd Report)," Bull. Japan Soc. of Prec. Eng., Vol. 9, No. 1. Veziroglu, T. N., 1967, "Correlation of Thermal Contact Conductance Ex-

perimental Results," presented at the AIAA Thermophysics Specialist Conference, New Orleans, LA, Apr. 17-20.

- \*Yovanovich, M. M., 1982, "Thermal Contact Correlations," Spacecraft Ra-

diative Transfer and Temperature Control, T. E. Horton, ed., Vol. 83 of Progress in Astronautics and Aeronautics, New York, pp. 83-95.

Yovanovich, M. M., DeVaal, J. W., and Hegazy, A. A., 1982, "A Statistical Model to Predict Thermal Gap Conductance Between Conforming Rough Surfaces," AIAA Paper No. 82-0888.